Photoreceptor encoding of supersaturating light stimuli in salamander retina

Jian Wei Xu, Mingli Hou and Malcolm M. Slaughter

Department of Physiology and Biophysics, University at Buffalo, 124 Sherman Hall, Buffalo, NY 14214, USA

In the dark-adapted salamander retina, spikes could be elicited from rods under normal physiological conditions. Spike activity was observed in rods during the recovery phase of the response to saturating light. These action potentials were calcium spikes, blocked by cadmium and L-type calcium channel blockers. In response to light stimuli that saturate the rod peak response, calcium action potentials occurred with a delay that depended on light intensity, with stronger light increasing spike latency. Therefore, these spikes encode rod visual information at light intensities beyond rod saturation. Postsynaptic currents of similar time course were observed in second and third order neurones. Since rods exposed to brighter light stimuli produced more delayed spike activity, these signals might contribute to negative afterimages.

Rod and cone photoreceptors in vertebrate retina encode visual information under different lighting conditions. Rods are a few orders more sensitive to light (McNaughton, 1990; Yang & Wu, 1997) and responsible for dim light vision. They saturate in a light range at which cones respond linearly to light (Yang & Wu, 1997). As light intensity increases, the peak current response of a rod saturates. Greater light intensities prolong the recovery of the rod current despite producing no further increase in peak response. Paradoxically, psychophysical studies have demonstrated that the rod pathway can still convey visual information when exposed to supersaturating light stimuli (Sakitt, 1975, 1976; Sakitt & Long, 1979; Adelson, 1982).

One phenomenon these studies concentrated on was the visual afterimage. A remarkable demonstration of this phenomenon, performed on human rod achromats, was to present a supersaturating test image on top of a dimmer, but still saturating background. The test image was invisible to the observer. However, if the subject's eye were subsequently closed, then a positive afterimage became discernable (Sakitt, 1976). Sakitt speculated that the supersaturated test image is stored within the phototransduction process in rod outer segments (Baylor & Fuortes, 1970). This storage is encoded in the rod although it cannot be relayed to the retinal network until the cessation of the image. The supersaturating stimulus is not encoded in the peak voltage response of the rod, but in the delayed recovery of the rod voltage response. Brighter stimuli produce more delayed rod recovery. Sakitt

postulated that the formation of positive afterimages was based on this increased latency of recovery of the rod response after a saturating light. The latency before the beginning of the recovery of the response depends on the incident light intensity (Penn & Hagins, 1972; Normann & Werblin, 1974; Yang & Wu, 1997) Rods illuminated by the higher intensity of the test signal had longer latencies than rods exposed to the background. A positive afterimage would occur if rods exposed to the test stimulus were more hyperpolarized than those exposed to the background stimulus. Consequently, Sakitt hypothesized that a positive afterimage could be formed in the time window when background rods recovered while test rods did not. This is because the rods responding to the test stimulus were less depolarized (slower to recover), and releasing less neurotransmitter, characteristics of brighter light and a positive image. If the intensities of the test and background stimuli were increased, it would take longer for a differential response of the affected rods. Thus, both the differential recovery and the positive afterimage are intensity dependent.

This model suggests the importance of rod responses to visual encoding during light exposure traditionally defined as saturating. The above model can explain the positive rod afterimage. However, the authors had difficulty explaining the origin of negative afterimages (Sakitt, 1976), which presumably also originate from photoreceptors. In this paper we report that rods can respond to saturating light with calcium action potentials during the recovery phase of the light response. These spikes encode the intensity

of supersaturating light stimuli. Furthermore, these spikes can potentially encode both positive and negative afterimages.

Methods

Preparations and recordings

Larval tiger salamanders were obtained from Kons Direct (Germantown, WI, USA) and Charles Sullivan (Nashville, TN, USA) and were kept in tanks maintained at 4°C on a 12 h light–dark cycle. Retinal slices were prepared as previously described (Wu, 1987; Awatramani & Slaughter, 2000). A few wholemount retinal experiments were performed. In these experiments the retina was placed photoreceptor side down over a ring of filter paper and then covered by another ring of filter paper. This left the central retina exposed, for both light stimulation and patch clamp recording. Both the retinal slice and the wholemount retina were superfused with oxygenated Ringer solution. All procedures were performed in accordance with the US Animal Welfare Act and the National Institutes of Health Guide for the Care and Use of Laboratory Animals (publication 85-23) and were approved by the University Animal Care Committee. All operations were performed
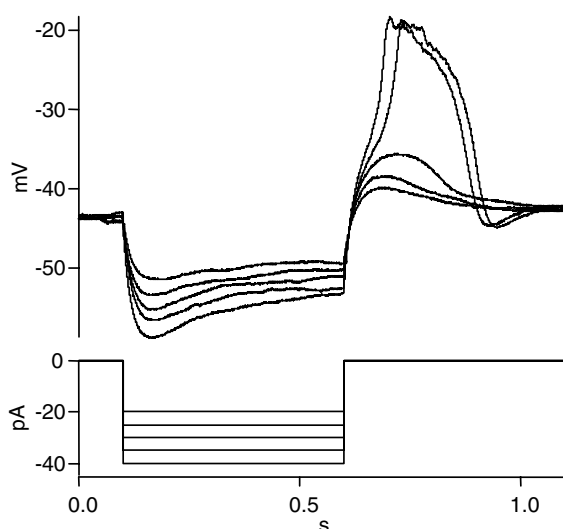
Figure 1. Anodal break excitation induces regenerative action potential in rods
A rod from a dark-adapted salamander retinal slice was current clamped and negative current steps of 500 ms were applied to the cell. The currents ranged from −20 to −40 pA in 5 pA increments. A depolarizing overshoot was present when the current injection ceased. When the overshoot reached a threshold, the depolarization became regenerative (cessation of currents of −35 and −40 pA). Larger negative currents produced faster regenerative depolarizations but the amplitudes remained the same. An undershoot was present at the end of the regenerative potentials, but not in traces which lacked a regenerative potential. Similar results were obtained in 5 other cells. In different cells the current values needed to generate regenerative potentials varied, ranging from −20 to −50 pA.

under infra-red illumination to keep the retina fully dark adapted.

Recordings were made using either the whole-cell ruptured patch technique or the gramicidin perforated patch method (Kyrozis & Reichling, 1995). The latter was used to preserve the cytosolic content of the cells. Second order neurones were identified by their response characteristics and their appearance after staining with Lucifer Yellow. Rods were identified by their outer segment. The slices were continuously bathed with control Ringer solution containing (mm): 111 NaCl, 2.5 KCl, 1.8 $CaCl_2$, 1 $MgCl_2$, 10 dextrose, and 5 Hepes, buffered to pH 7.8. The recording pipette contained (mm): 100 potassium gluconate, 5 NaCl, 2 $MgCl_2$, 5 EGTA, 5 Hepes and 0.1% Lucifer Yellow, buffered to pH 7.4 with KOH. In perforated patch recordings, 5 mg of gramicidin was dissolved in 1 ml DMSO and 2.5 μl of it was added to 1 ml of pipette solution. The pipette solution containing gramicidin was sonicated before use. In whole-cell ruptured patch recordings, the solution also contained an 'ATP regenerating cocktail' consisting of 4 mm ATP, 20 mm phosphocreatine and 50 units ml^{-1} creatine phosphokinase.

Electrophysiological data were collected with a List EPC-9 amplifier, HEKA Pulse software and a Macintosh G3 computer and analysed with Igor Pro software. The analog signals were filtered at 5 kHz. Data are expressed as means ± s.e.m. Access resistance was 8–15 MΩ for whole-cell rupture recordings and 8–30 MΩ for perforated patch recordings and generally was not compensated. Liquid junction potential for whole-cell rupture recording was measured to be around −10 mV and this value adjustment was applied to all the data. No liquid junction potential adjustment was made for perforated patch recordings.

Light responses were generated by either a green (wavelength 500 nm) or a red (wavelength 650 nm) LED. The light intensity units used in the text only apply to the green light stimuli and defined such that 1 unit of light is equivalent to an intensity $\sim 10^3$ photons $\mu m^{-2} s^{-1}$.

Results

Anodal break excitation was used to demonstrate that rods possess voltage-gated channels that can generate action potentials under normal physiological conditions (Fig. 1). Rods in the dark-adapted salamander retinal slice were recorded in current clamp mode, typically by the whole-cell ruptured patch method. The mean dark membrane voltage of rods under such conditions (whole-cell recording and potassium gluconate internal solution) was −41.8 ± 2.8 mV ($n = 36$).

Steps of negative current were injected to hyperpolarize the rod (Fig. 1). The current steps ranged from −20 to −40 pA, and lasted for 0.5 s. The current induced a peak

hyperpolarization that decayed during the pulse, probably due to activation of I_h current (Bader & Bertrand, 1984; Barnes & Hille, 1989). When the current injection was terminated, the cell rapidly depolarized and overshot the resting potential, probably due to I_h and voltage-activated calcium channels. The overshoot eventually decayed to the resting dark potential, due in part to the deactivation of I_h, inactivation of calcium current, and activation of calcium-dependent potassium and chloride currents.

During the offset of a larger negative current (-35 pA), an inflection appeared in the depolarizing voltage response, followed by a spike. The membrane voltage rose rapidly to a voltage more positive than -20 mV. Increasing the current injection to -40 pA resulted in a faster depolarization at current offset. The spike was of similar amplitude, although it reached peak earlier. After the peak of the spike, the membrane potential decayed gradually for about 50 ms. Then the voltage decline became more rapid and eventually led to an undershoot. The undershoot was not present in traces without spikes. The undershoot was probably caused by the activation of calcium-dependent K^+ and Cl^- currents, because these two ions had reversal potentials more negative than the rod membrane potential under our experimental conditions.

These experiments indicate that voltage-gated ion channels in the inner segment and terminal of the rod can, under certain conditions, produce regenerative depolarizations. Regenerative currents have been reported in salamander and lizard cones (Maricq & Korenbrot, 1988; Barnes & Deschenes, 1992), produced by the combination of calcium current and calcium-activated chloride current (the chloride reversal potential was set to 0 mV in the cited experiments). However, the chloride reversal potential was set at -65 mV in our experiments and did not contribute to the generation or maintenance of the regenerative response shown in Fig. 1. On the contrary, it may contribute to the decline and collapse of the overshoot. The only significant depolarizing current in our experiments was the calcium current. It is likely that the calcium current is regenerative due to its high density at the synaptic terminal of rods (Xu & Slaughter, 2005).

Action potentials can also be produced by bright light. Dark-adapted rods were recorded in current clamp mode. Of the rods examined, about a fourth (18 out of 78) exhibited spike activity during the recovery phase of the light response (Fig. 2). The spike occurred several seconds after the offset of a 1 s light stimulus (Fig. 2A). The spikes had different shapes in different cells, as exemplified in Fig. 2. The depolarization reached approximately the same voltage, with a mean peak potential of -25.7 ± 2.7 mV ($n = 18$). The timing of the start of the regenerative potential ranged from 8 to 12 s after the light stimulus, with a mean of 10.1 ± 1.5 s at a light intensity of 1.3 log units (see Methods). We show below that the delay depends on the incident light intensity.

Regenerative potentials have been recorded in rods during the recovery phase of the light response when the retina was treated with TEA to block potassium channels (Fain & Quandt, 1980; Fain et al. 1980). A prolonged depolarization was also observed in rods after injection of brief depolarizing current pulses in cells with high internal chloride (Thoreson & Burkhardt, 1991; Burkhardt et al. 1991). In 20% of cones in turtle retina, feedback from horizontal cells evokes a spike (Piccolino & Gerschenfeld, 1980). Transretinal current pulses also induced oscillatory depolarizations in frog retina (Miyachi et al. 1984). In our
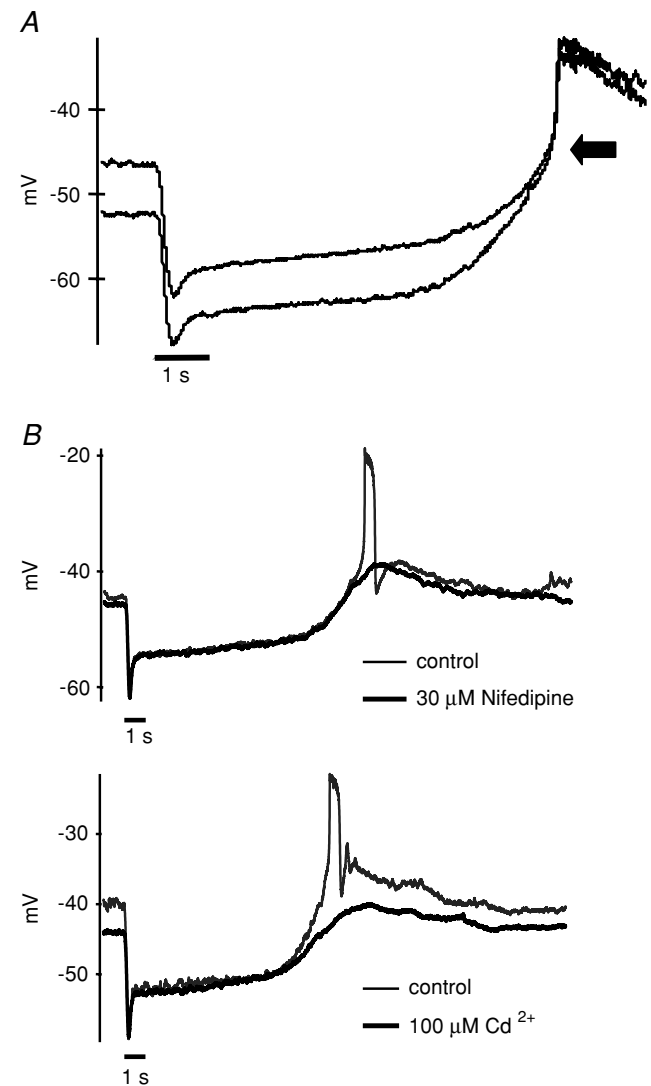
Figure 2. The regenerative potentials are light-driven calcium spikes

A, a 1 s bright light stimulus produced a delayed action potential in a current clamped rod (0 pA). This spike amplitude was similar if the rod was hyperpolarized by injecting negative current. B, the light-induced regenerative potentials were blocked by Ca^{2+} channel blockers: 30 μM nifedipine (upper trace) or 100 μM Cd^{2+} (lower trace). The black bars below the voltage traces represent 1 s light stimuli.

recordings, the retinal slice was superfused with control Ringer solution and no current injection was applied (Fig. 2*A*). This indicates, for the first time, that regenerative potentials occur in the rod light response under normal physiological conditions.

Fain *et al.* (1980) concluded that the regenerative potentials recorded in toad rods in the presence of TEA represented calcium currents, which only became regenerative after the potassium conductance was blocked. The regenerative potentials we observed under normal physiological conditions were also calcium currents because they were blocked by 100 μM Cd^{2+}, a blocker of voltage-gated calcium channels, or 30 μM nifedipine, an L-type calcium channel blocker (Fig. 2*B*). They cannot be calcium-dependent potassium or chloride currents, since both have more negative equilibrium potentials.

Rod spikes were detected without blockade of potassium channels in our experiments.

Nevertheless, both voltage-dependent and calcium-dependent (BK) potassium channels limited the amplitude and duration of rod spikes. Rods exhibit a large BK current (Bader & Bertrand, 1984; Moriondo *et al.* 2001; Xu & Slaughter, 2004). When the BK channel was blocked by 1 mM TEA, the regenerative potential reached a mean peak amplitude of -15.4 ± 3.7 mV ($n = 5$), compared with -25.7 ± 2.7 mV under control conditions (Fig. 3*A*). Similar results were obtained using 100 nM charybdotoxin, another BK channel blocker. In two cells, the oscillatory potentials became fewer and broader (Fig. 3*A* upper panel). However, in other cells the spike amplitude increased without a notable broadening (e.g. Fig. 3*A* lower panel). Thus, in rods as in other neurones the BK channels
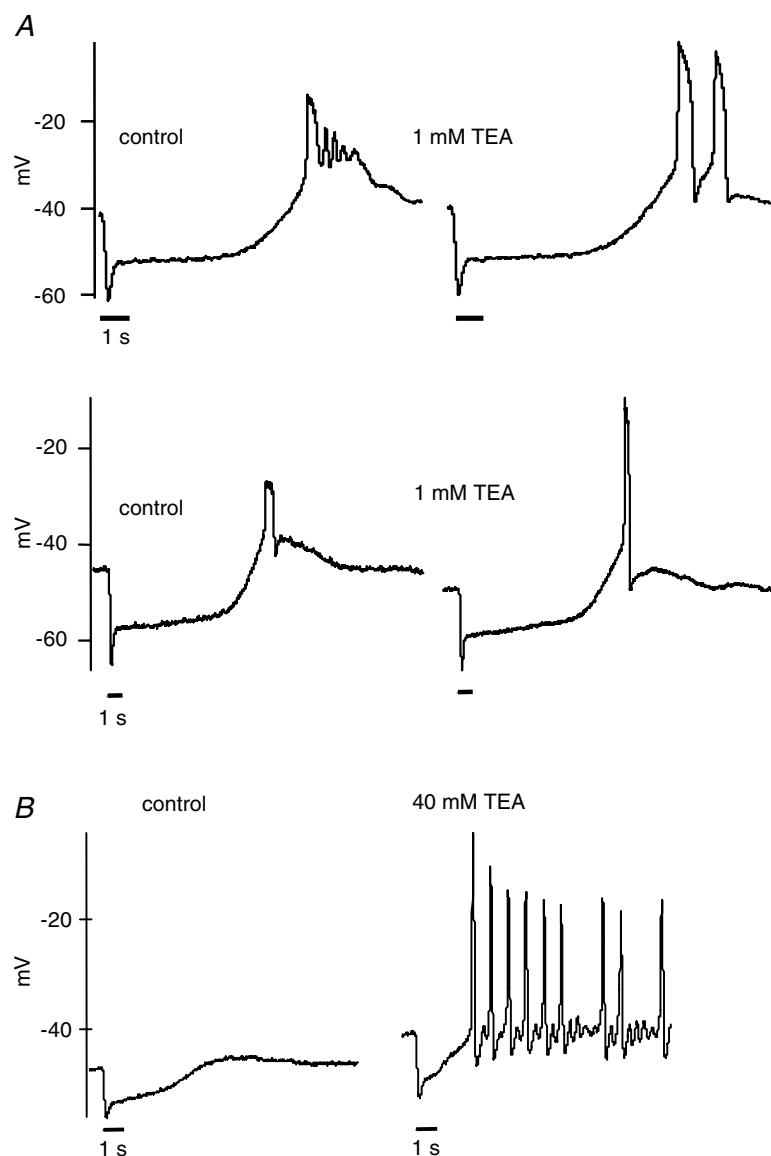
Figure 3. Potassium channels limit the amplitude of the calcium spike
A, the Ca^{2+} spikes reached more depolarized voltages when large conductance Ca^{2+}-activated potassium (BK) channels were blocked by 1 mM TEA. The average peak in the presence of TEA was -15.4 ± 3.7 mV ($n = 5$) compared with -25.7 ± 2.7 mV ($n = 18$) in control conditions. The spike frequency was sometimes affected by BK channel block (upper trace). *B*, blocking voltage-gated potassium channels induced regenerative potentials in rods. A rod was stimulated by light under control conditions and after treatment of the retinal slice with 40 mM TEA. The block of potassium channels induced spontaneous oscillatory action potentials (right) that could be suppressed by light. In 6 rods, the action potentials had a mean peak of -6 ± 4 mV in the presence of 40 mM TEA. A light stimulus of 1 s is indicated by the bar below the voltage traces.

produce a negative feedback that limits the size of the calcium spike (Hille, 2001).

Voltage-gated potassium channels found in rods further limited the amplitude of spike depolarization (Attwell & Wilson, 1980; Barnes, 1994). When 40 mM TEA was applied, the regenerative potential reached a mean peak amplitude of -6 ± 4 mV ($n = 6$) (Fig. 3B). In the presence of 40 mM TEA, the regenerative spikes became spontaneous at the dark membrane potential of rods and the spikes were only suppressed by light-induced hyperpolarization. Calcium-dependent chloride channels may contribute to the recovery of calcium spikes under these conditions. Our results demonstrate that, at least in some rods, the voltage-gated calcium current is sufficiently large that it can overcome hyperpolarizing currents, yielding a regenerative response under physiological conditions.

The calcium current can be observed in the I–V responses of rods under normal conditions, without the need to block potassium channels (Fig. 4). The I–V curve was obtained by a voltage ramp from -70 mV to 0 mV at 0.5 mV ms^{-1}, recorded in control Ringer solution. The I–V curve was linear from -70 mV to about -35 mV, at which point an inward current was activated. It peaked at around -25 mV. This current could be blocked by 50 μM Cd^{2+}, indicative of a calcium-dependent inward current. It can only be calcium current, because calcium-activated K^{+} and Cl^{-} currents are both outward in this voltage range. This result is consistent with the previous experiments showing that the calcium current is regenerative, even in the presence of outward currents.

The I–V curve exhibits two stable states, which can account for the regenerative calcium spikes in rods (Fig. 4, lower panel). A stable state is a zero current crossing point at which depolarization produces an outward current and a hyperpolarization produces an inward current. Thus, voltage excursions around the stable state produce currents that restore the rod's potential to the stable state. A segment of the I–V curve from the upper panel was smoothed through a box filter and expanded. There are three points along the I–V curve that cross the zero current line: A, B and C. However, only A and B are stable states. Points D–G are arbitrary voltages and the arrows indicate the directions of voltage change at these points. Point C, which intersects the zero current axis, is not a stable state but is important because it is the threshold for the regenerative potential.

It can be inferred from the model that if the rod depolarizes to threshold (point C in Fig. 4), then the depolarization will become regenerative. What is the source of the inward current that brings the rod to threshold? Figure 1 suggests that anodal break excitation contributes to it, indicating the contribution of voltage-gated channels. To examine if any voltage-independent mechanism might contribute to it, we recorded the light response of a rod in voltage clamp mode. Light onset produced an outward current.

At light offset, the rod produced an inward current undershoot (Fig. 5A, V_{hold} was -40 mV). As the light intensity increased, the undershoot increased in amplitude and peaked later. If the light intensity is big enough, it may produce enough inward current to bring the rod to spike threshold. To test this, we compared the light-evoked current in a rod with spike generation in the same rod (Fig. 5B). The time course of the light-evoked inward current (below baseline, dotted line) corresponded with the rod depolarization (above resting potential). The spike in the rod occurred near the peak of the inward current. Thus, the undershoot is the spike generator. It is likely to be augmented by voltage-gated channels such as I_h. This inward current was also seen when gap junctions were blocked by carbenoxolone ($n = 3$), so it is not the result of gap junction currents from neighbouring rods.
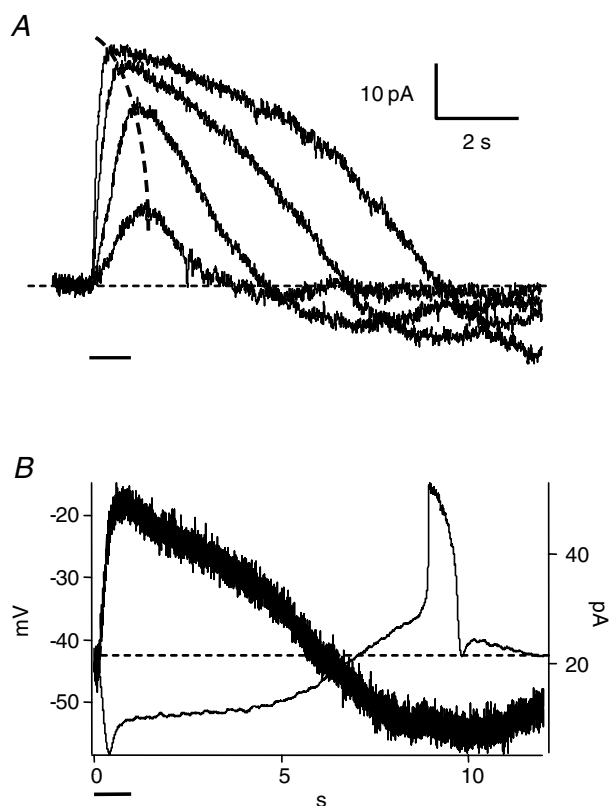
Torre and coauthors found a current undershoot in rods when the cytoplasm was dialysed with BAPTA,
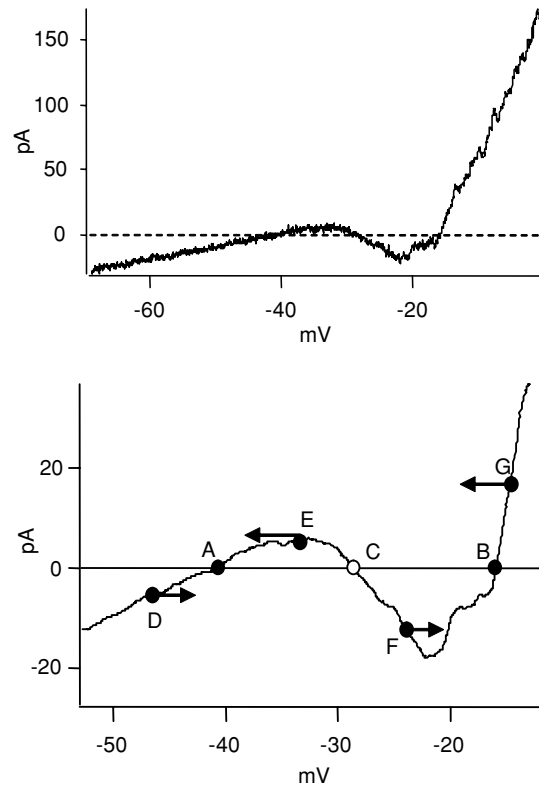
Figure 4. A bi-stable state in rods is responsible for the regenerative potentials

A, the I–V curve of the rod was obtained by a voltage ramp from -70 to 0 mV at 0.5 mV ms^{-1}. From -70 to -35 mV, the I–V curve was linear. At -35 mV, an inward current was activated. It reached its peak at around -20 mV and then an outward current dominated the net current. B, part of the I–V curve from A was filtered and expanded. The I–V curve crossed the 0 current line at points A, B and C. A and B are stable states, C is not. D–F are arbitrary points and the arrows indicate the direction of potential change when the rod voltage is at any of these points. As illustrated, C is the threshold for the regenerative potential, and B is the peak of the regenerative potential.

thus affecting cGMP phosphodiesterase activity (Torre *et al.* 1986). Perhaps our experiments, in which internal solution contains 5 mM EGTA, changed the native calcium buffering properties of rods and hence affected its response. We recorded rod light responses using the gramicidin perforated patch method to preserve the internal content of rods (Fig. 5*A*). The undershoot was present in these perforated patch voltage clamp recordings (3 in 10). As in experiments using ruptured patches, the undershoot occurred in some rods but not in others. The presence of an undershoot was consistent in a given animal; most rods in the same retina either had an undershoot or did not. An undershoot was observed in rods in about 25%

of retinal slices (7 in 30), consistent with the percentage of spike generation recorded in current clamp mode. Thus the undershoot during the recovery of the light response was not an artifact of internal cell dialysis.

In the rod depicted in Fig. 5*A*, the recovery phase of the rod current had a slight undershoot when the incident light intensity was low. At higher light intensities, the undershoot became bigger. The amplitude and timing of the undershoot correlated with light intensity. The stronger the light signal, the later the peak of the undershoot. This indicates that the undershoot can carry information encoding light intensity when the initial rod light response has saturated.

If the undershoot in the rod current varied with light intensity and was responsible for the generation of the calcium spike, it implies that the spike is intensity dependent. This is indeed the case, as illustrated in Fig. 6. In recordings of rod voltage, dim lights produced a very small voltage overshoot, equivalent to an undershoot in the current recordings. As the light intensity increased, the voltage overshoot became larger and eventually led to a calcium spike. Further increases in light intensity produced spikes of similar amplitudes, but longer latencies. The last four traces represent increasing intensities of supersaturating light stimuli, yielding calcium spikes of increasing latencies. Thus, the rod was able to encode light intensities that exceeded saturation. Similar results were observed in three cells.

The rod action potential is conveyed through the retinal network. Horizontal cells are postsynaptic to rods at

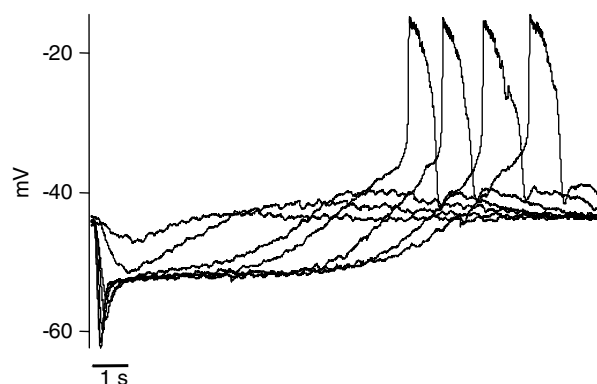**Figure 5. A voltage-independent current undershoot generates the action potential**
A, the light response of a rod in the dark-adapted retinal slice was recorded in voltage clamp mode using the gramicidin perforated patch method to preserve the internal content of the cell ($V_m = -40$ mV). The light intensities used were 0.08, 0.8, 1.3 and 1.7 log units (see Methods). Current undershoots were induced by light during the recovery phase at all intensities, but barely noticeable at the lowest light intensity. As light intensity increased, the amplitude and time to peak of the undershoot both increased. The dashed line connects the peak of the light responses. *B*, the light responses of the same rod in voltage clamp (thick trace) and current clamp (thin trace) mode induced by the same light stimulus were overlaid. The voltage overshoot and Ca^{2+} action potential were induced during the recovery phase. In the current trace, no action potential was induced because the voltage of the cell was clamped to -40 mV but a current undershoot was evident below the baseline (dashed line).


Figure 6. Action potential latency is light-intensity dependent
A rod was current clamped (0 pA) and light stimuli of increasing intensities were applied in a dark-adapted retinal slice. The interval between stimuli was 40 s. The stimulus intensities were -0.7, 0.08, 0.8, 1.3 and 1.7 log units (see Methods). Stronger light intensity prolonged the recovery phase of the light response and the onset of the rod action potential. At lower light intensities the Ca^{2+} action potential was not present, though slight overshoots were present during the recovery phase of the light response. The overshoot became larger with increasing light intensity and the Ca^{2+} action potential occurred at threshold. The Ca^{2+} action potentials had similar peak amplitude and kinetics.

a glutamatergic synapse. If the retina was exposed to light while recording the voltage-clamped currents of a horizontal cell, spike-like oscillatory inward currents were observed with a time course similar to the regenerative potentials of rods (Fig. 7*A*). The horizontal cell shown in the figure received both rod and cone input. The immediate decline in outward current at the end of the 1 s light stimulus represents cone input (Yang & Wu, 1996). The prolonged outward current after the initial drop (arrow) reflects the rod afterpotential. About 12 s after the offset of the stimulus, oscillatory inward currents appeared. The current polarity and time course matched the depolarizing regenerative potential in rods. In 3 out of 10 horizontal cells that received prominent rod input, oscillatory inward currents were observed with a time course ranging from 8 to 15 s after onset of the light response. The same phenomenon was also found in third order neurones. Figure 7*B* shows light-evoked IPSCs of an amacrine cell. In five consecutive traces, in addition to the short latency on–off response induced by the light stimulus, a late response was observed about 8 s after the offset of the light stimulus. Three of 11 amacrine cells showed delayed responses. To determine if delayed light responses were an artifact of the retinal slice preparation, a few experiments were performed in the retinal wholemount preparation and a similar phenomenon was observed. An example is shown in Fig. 7*C*, which is a recording from a sustained On ganglion cell clamped at −70 mV. A 1 s light stimulus produced a sustained On and a transient Off light response, which was followed approximately 8 s later by a pair of fast inward currents. There have been previous reports of delayed light responses in third order neurones in other vertebrate retinas (Chino & Sturr, 1975*a,b*; Zeise & Hamdorf, 1983). These prior studies also suggested that rods initiated the delayed light response, although direct recordings of rod light responses were not obtained.

What physiological functions do these regenerative potentials perform? The regenerative potentials occur after a relatively strong light stimulus. Often the calcium spikes produce a prolonged plateau depolarization of rods. Is the rod responsiveness increased or decreased during this plateau? To test this, we applied strong light stimuli at different intervals. Figure 8 shows the light response of a rod in which regenerative potentials occurred about 10 s after the offset of the light stimulus. A second light stimulus at the same intensity was applied 45 s after the first light stimulus, giving the cell enough time to relax to the baseline, and an identical response was induced. However, if the second light stimulus was applied at a time that coincided with the regenerative potential, then the second response to a saturating light was bigger because the membrane voltage of the cell had not relaxed to baseline (Fig. 8*B*). This enhancement does not indicate a change in light sensitivity; it reflects the enhanced voltage range of the rod when it has been depolarized. On the other hand,
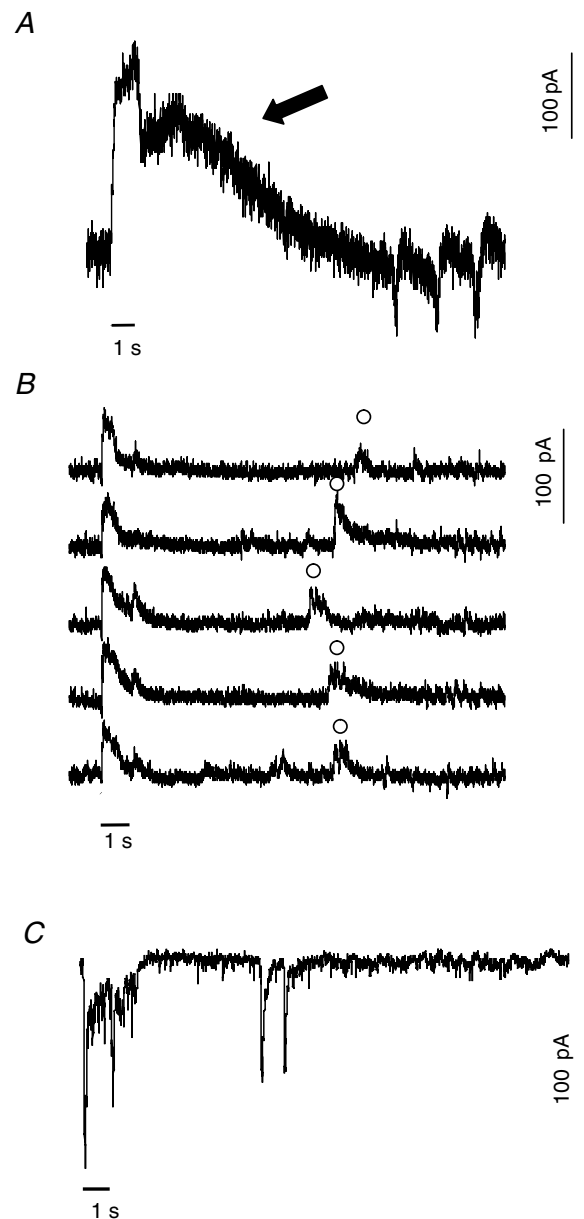
Figure 7. Delayed light responses are observed in second and third order neurones with a time course similar to rod spikes
A, a light-evoked EPSC was recorded from a horizontal cell in the dark-adapted retinal slice ($V_m = -50$ mV). In response to a 1 s red light stimulus (black bar) the recovery phase consisted of a fast cone and slower rod signal (arrow). About 12 s after the onset of the light stimulus, spike-like negative (inward) currents appeared. Delayed inward currents were seen in 3 out of 10 horizontal cells with a delay of 10.1 ± 2.1 s after light onset. *B*, light-evoked IPSCs were recorded from an amacrine cell in a dark-adapted retinal slice ($V_m = -10$ mV). There were On and Off responses at onset and offset of the light stimuli. A delayed response (O) was observed in each of a series of traces. The bar represents light stimuli of 1 s. *C*, in the dark-adapted wholemount retina, EPSCs were recorded from a ganglion cell clamped to −70 mV and stimulated with a bright, 1 s light. Two delayed EPSCs occurred after the cessation of the light response.

if a second saturating light stimulus was applied a few seconds after the first one, before the rod recovered to its baseline dark membrane potential, then the light response was smaller than control. The enhancement occurred at the time of the regenerative potential, not earlier or later, indicating it was not due to the adaptation state of the retina. Similar results were obtained in four rods. The results suggest that at high light intensities, rods have a resonant frequency at which the voltage response to repetitive light stimuli is maximal. Responses to light stimuli of higher frequencies are decreased. Responses to lower frequency light stimuli are unchanged. These properties make the rod a band pass filter at high light intensities. Furthermore, the stronger the light intensity, the longer it takes for the regenerative potential or undershoot to occur, and hence the lower the resonant frequency. The enhancement of the rod signal at a resonant frequency is contributed to by both the biochemical process in the outer segment and the voltage-dependent channels in the remainder of the rod. Both are required. If the cell is depolarized by injecting a standing positive current, the light response is enhanced but the hyperpolarization does not reach the same potential (Fig. 8*A*).

Discussion

Physiology of the rod calcium spike

Generally, first and second order neurones of vertebrate retina are regarded as non-spiking neurones. However, Ca^{2+} action potentials have been observed in isolated retinal bipolar cells (Zenisek & Matthews, 1998; Ma & Pan, 2003). Additionally, a population of rat cone bipolar cells have a high density of voltage-gated sodium channels (Pan & Hu, 2000) and sodium spikes have also been reported in photoreceptors (Kawai *et al.* 2001). Light signals can induce calcium spikes in bipolar cells and they are proposed to boost small light signals at the synaptic terminal (Zenisek & Matthews, 1998; Protti *et al.* 2000; Ma & Pan, 2003).

The rod calcium spike functions at the other extreme of light stimulation. The timing of regenerative potentials encodes light information when the intensity is strong enough to saturate the peak response of rods. The prolonged undershoot after an intense light stimulus can produce a positive afterimage (Sakitt, 1976). This is because the rods exposed to the strongest lights are hyperpolarized longer and release less transmitter. These rods
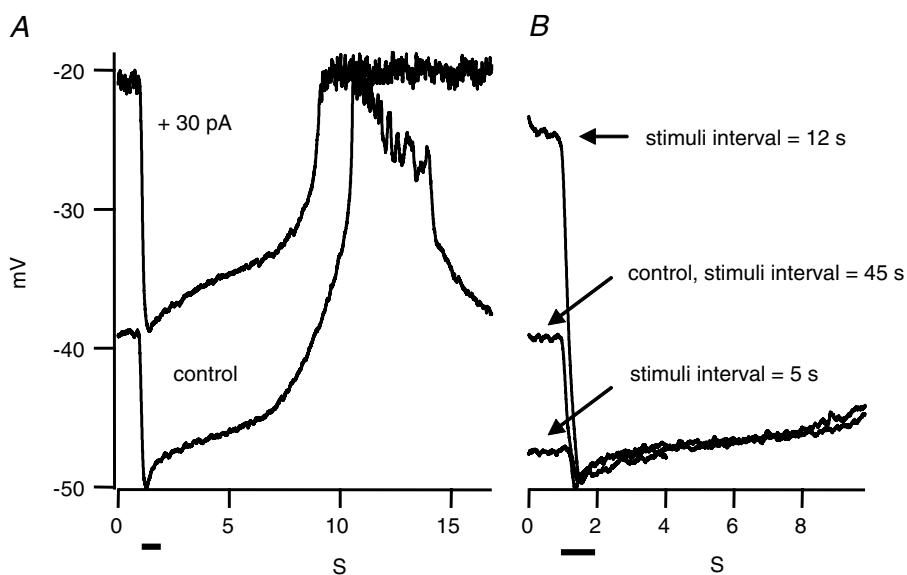
Figure 8. Frequency response due to the rod action potential
A, the control trace shows the light response of a rod in a dark-adapted retinal slice and the calcium action potential. A 30 pA continuous positive current injection depolarized the cell to −20 mV, about the same voltage as that of the peak of the Ca^{2+} action potential. The amplitude of the light response was increased by the current injection but the peak of the light-evoked hyperpolarization did not reach the control potential. *B*, in the same rod, paired light stimuli were given at different interstimulus intervals. If the interval was about the same as the time from the onset of the stimulus to the plateau of the Ca^{2+} action potential (12 s in this case), the cell was more depolarized than baseline during the second stimulus and the light response was about 2.5-fold larger than control. When the interval was shorter than 12 s, such as 5 s in this example, the cell did not recover to baseline and consequently the light response was reduced. After a long interstimulus interval (45 s), the rod voltage returned to control levels and the second light stimulus was the same as the first. The bars represent the 1 s light stimuli.

encode a 'light' signal while rods exposed to less light have recovered and transmit a 'dark' signal.

The depolarizing overshoot and spike can produce a negative afterimage, since these rods are releasing more transmitter and therefore encoding a 'darker' signal. This suggests the following model. If rods are stimulated by a saturating test stimulus that is brighter than a background stimulus to adjacent rods, then the test rods are initially more hyperpolarized than adjacent rods, release less transmitter, and therefore encode a 'brighter' signal than background rods. Correspondingly, the background rods depolarize earlier and therefore may have an earlier spike, which again would represent a positive afterimage in the test rods. These signals produce the positive afterimage. However, after a further delay the test rods depolarize and produce a voltage overshoot and spike, they release more transmitter than the background rods, and therefore now the test stimulus is encoded as 'darker', the opposite of the original signal and therefore a negative afterimage. If no overshoot occurs during the recovery phase of rod light response, then only a positive afterimage occurs. When there is a voltage overshoot and regenerative depolarization, a negative afterimage could occur after the positive image (Fig. 9).

The regenerative depolarization sets the rod at voltages more positive than the resting dark membrane potential. During the period of the voltage overshoot, the rod is able to produce larger light responses. Similar short-term potentiation due to an off voltage overshoot was reported in salamander and turtle horizontal cells (Wu, 1988; Akopian *et al.* 1991). This type of potentiation of the rod signal requires the light stimulus to follow a specific temporal frequency, determined by stimulus intensity. Stimuli at the resonant frequency activate the rod during the regenerative depolarization and are enhanced. The higher the light intensity, the lower the resonant frequency. While the voltage overshoot creates a very low frequency bandpass filter at high light levels, the rod synapse produces a higher frequency bandpass filter presumably optimized for dim light intensities (Armstrong-Gold & Rieke, 2003).

Detection of rod action potentials

In this study, we show for the first time that regenerative potentials can be observed in rods during the recovery phase of the light response under normal physiological conditions. However, regenerative potentials were only observed in about 25% of rods, although calcium spikes could be induced in all rods by blocking potassium channels with 40 mM TEA. Perhaps the state of individual retinas determined whether we would observe rod spiking. Though we dark-adapted the animals before all experiments, the process of making the retinal slice may have exposed the retina to a small amount of light. Therefore it is possible that retinas were in different adaptational states. This might explain why we consistently observed rod spikes in some retinas and not in others.

Although rod calcium spikes have not been reported before under normal physiological conditions, it is not likely to be an artifact of our procedures. We obtained the same results when using the less invasive gramicidin perforated patch method and we observed transynaptic events that corresponded to rod spikes. There have been other reports of delayed light responses, appearing from 2 to 10 s after offset of a light stimulus, in turtle and frog retina (Chino & Sturr, 1975*a*,*b*; Zeise & Hamdorf, 1983; Protti *et al.* 2000). These signals were proposed to originate in the rod. In addition, field potential recordings have detected an e-wave that has the same temporal properties and intensity sensitivity as the rod spike (Newman & Lettvin, 1978). It is likely that the whole-cell recording technique, as compared with previous sharp electrode recordings, allowed for the detection of calcium spikes by reducing leak. Blocking potassium channels, which decreases membrane conductance and increases rod excitability, always induces spontaneous calcium spikes (Fain *et al.* 1980) (also see Fig. 3). This indicates that all rods are capable of spike formation.

The source of the current undershoot was not determined. Torre and colleagues found that the current response of a rod to light had a prominent undershoot when a high concentration of Ca^{2+} buffer (10 mM BAPTA) was present in the cytoplasm, but not in control conditions (Torre *et al.* 1986). A conclusion from their work was that
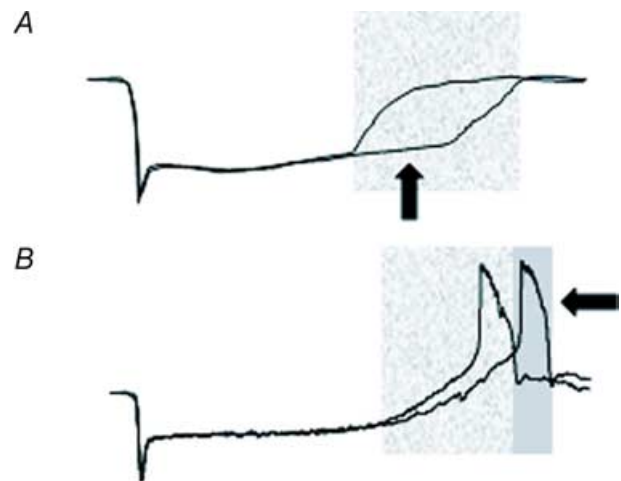
Figure 9. Model of rod afterimage formation
A, the voltage response of a rod is shown when exposed to two different light intensities, both of which saturate the peak rod response. In the highlighted region, the rod response to the brighter stimulus remains hyperpolarized (darker trace, arrow), which encodes light on. This would create a positive afterimage. *B*, the same protocol is used in a spiking rod. In the second highlighted region, the rod exposed to the higher light intensity produces a delayed spike (arrow), encoding darkness. This would create a negative afterimage of the light stimulus.

a slowing of calcium changes in the outer segment of isolated rods could produce a current undershoot. Our results show that when using perforated patch method, which presumably maintained the internal Ca^{2+} buffers of the cell, the undershoot was still observed (Fig. 5). The reason for this discrepancy is not clear. One piece of evidence showing that the rod's internal content was conserved during the perforated patch recording was that the time to peak of the current response to increasing intensities of light decreased (dashed line in Fig. 5*A*) (Baylor & Hodgkin, 1974; Baylor *et al.* 1979). This was also seen in Torre's study in the control responses (Torre *et al.* 1986, Lamb *et al.* 1986). The undershoot they observed was much larger than the one seen in our experiments, but it did show a light intensity-dependent delay. It is possible that rods *in situ* do not have the same transmembrane calcium flux and that slows calcium changes in the outer segment, accounting for the current undershoot in our experiments. Alternatively, a voltage-independent process in the inner segment may be responsible for the current undershoot.

Repolarization after the calcium spike

What accounts for the repolarization of the calcium spike? Large conductance Ca^{2+}-activated potassium channels contribute to the shape of spikes (Fig. 3). However, blocking the BK channels had no consistent effect on the length of the action potentials (Fig. 3). It is possible that other potassium channels turn off the Ca^{2+} action potentials. However, when almost all the potassium currents in rods are blocked, Ca^{2+} action potentials are spontaneous and oscillatory (Fig. 2*B*). Therefore K^+ channels are not necessary for repolarization of Ca^{2+} action potentials. Calcium-activated chloride current is not necessary for repolarization either because the oscillatory spikes are also observed in gramicidin perforated patch recordings that preserve the Cl^- concentration inside the cell. In salamander rods, the Cl^- reversal potential is about -20 mV (Thoreson *et al.* 2002) and hence not hyperpolarizing. Fain and coauthors also found that the Cl^- conductance had no effect on the Ca^{2+} spike oscillation (Fain *et al.* 1980). Therefore the most likely candidate is the Ca^{2+} channel itself. The L-type Ca^{2+} channels in retinal photoreceptors are traditionally regarded as having little or no voltage-dependent inactivation (Corey *et al.* 1984; von Gersdorff & Matthews, 1996). However, in a recent study, Rabl and Thoreson found that rod Ca^{2+} channels inactivate substantially during depolarization (Rabl & Thoreson, 2002). A 5 s depolarization to -20 mV inactivated more than 70% of the Ca^{2+} current in isolated rods. They also showed that local depletion of Ca^{2+} ions in the synaptic cleft contributes to a transient decrease of Ca^{2+} current. These two factors may account for, or contribute

to, the repolarization of the Ca^{2+} action potentials. They may also create a refractory period for the generation of another Ca^{2+} action potential.

References

Adelson EH (1982). The delayed rod afterimage. *Vision Res* **22**, 1313–1328.

Akopian A, McReynolds J & Weiler R (1991). Short-term potentiation of off-responses in turtle horizontal cells. *Brain Res* **546**, 132–138.

Armstrong-Gold CE & Rieke F (2003). Bandpass filtering at the rod to second-order cell synapse in salamander (Ambystoma tigrinum) retina. *J Neurosci* **23**, 3796–3806.

Attwell D & Wilson M (1980). Behaviour of the rod network in the tiger salamander retina mediated by membrane properties of individual rods. *J Physiol* **309**, 287–315.

Awatramani GS & Slaughter MM (2002). Origin of transient and sustained responses in ganglion cells of the retina. *J Neurosci* **20**, 7087–95.

Bader CR & Bertrand D (1984). Effect of changes in intra- and extracellular sodium on the inward (anomalous) rectification in salamander photoreceptors. *J Physiol* **347**, 611–631.

Barnes S (1994). After transduction: response shaping and control of transmission by ion channels of the photoreceptor inner segments. *Neuroscience* **58**, 447–459.

Barnes S & Deschenes MC (1992). Contribution of Ca and Ca-activated Cl channels to regenerative depolarization and membrane bistability of cone photoreceptors. *J Neurophysiol* **68**, 745–755.

Barnes S & Hille B (1989). Ionic channels of the inner segment of tiger salamander cone photoreceptors. *J Gen Physiol* **94**, 719–743.

Baylor DA & Fuortes MG (1970). Electrical responses of single cones in the retina of the turtle. *J Physiol* **207**, 77–92.

Baylor DA & Hodgkin AL (1974). Changes in time scale and sensitivity in turtle photoreceptors. *J Physiol* **242**, 729–758.

Baylor DA, Lamb TD & Yau KW (1979). The membrane current of single rod outer segments. *J Physiol* **288**, 589–611.

Burkhardt DA, Zhang SQ & Gottesman J (1991). Prolonged depolarization in rods in situ. *Vis Neurosci* **6**, 607–614.

Chino YM & Sturr JF (1975*a*). The time course of inhibition during the delayed response of the on-off ganglion cell in the frog. *Vision Res* **15**, 185–191.

Chino YM & Sturr JF (1975*b*). Rod and cone contributions to the delayed response of the on-off ganglion cell in the frog. *Vision Res* **15**, 193–202.

Corey DP, Dubinsky JM & Schwartz EA (1984). The calcium current in inner segments of rods from the salamander (*Ambystoma tigrinum*) retina. *J Physiol* **354**, 557–575.

Fain GL, Gerschenfeld HM & Quandt FN (1980). Calcium spikes in toad rods. *J Physiol* **303**, 495–513.

Fain GL & Quandt FN (1980*b*). The effects of tetraethylammonium and cobalt ions on responses to extrinsic current in toad rods. *J Physiol* **303**, 515–533.

Hille B (2001). *Ionic Channels of Excitable Membranes*, 3rd edn. Sinauer Associates, Sunderland, MA, USA.

Kawai F, Horiguchi M, Suzuki H & Miyachi E (2001). Na^+ action potentials in human photoreceptors. *Neuron* **30**, 451–458.

Kyrozis A & Reichling DB (1995). Perforated-patch recording with gramicidin avoids artifactual changes in intracellular chloride concentration. *J Neurosci Meth* **57**, 27–35.

Lamb TD, Matthews HR & Torre V (1986). Incorporation of calcium buffers into salamander retinal rods: a rejection of the calcium hypothesis of phototransduction. *J Physiol* **372**, 315–349.

Ma YP & Pan ZH (2003). Spontaneous regenerative activity in mammalian retinal bipolar cells: roles of multiple subtypes of voltage-dependent Ca^{2+} channels. *Vis Neurosci* **20**, 131–139.

McNaughton PA (1990). Light response of vertebrate photoreceptors. *Physiol Rev* **70**, 847–883.

Maricq AV & Korenbrot JI (1988). Calcium and calcium-dependent chloride currents generate action potentials in solitary cone photoreceptors. *Neuron* **1**, 503–515.

Miyachi E, Takahashi K & Murakami M (1984). Electrically evoked calcium responses in rods of the frog retina. *Jpn J Physiol* **34**, 307–318.

Moriondo A, Pelucchi B & Rispoli G (2001). Calcium-activated potassium current clamps the dark potential of vertebrate rods. *Eur J Neurosci* **14**, 19–26.

Newman EA & Lettvin JY (1978). Relation of the epsilon-wave to ganglion cell activity and rod responses in the frog. *Vision Res* **18**, 1181–1188.

Normann RA & Werblin FS (1974). Control of retinal sensitivity. I. Light and dark adaptation of vertebrate rods and cones. *J Generalphysiol* **63**, 37–61.

Pan ZH & Hu HJ (2000). Voltage-dependent Na^+ currents in mammalian retinal cone bipolar cells. *J Neurophysiol* **84**, 2564–2571.

Penn RD & Hagins WA (1972). Kinetics of the photocurrent of retinal rods. *Biophys J* **12**, 1073–1094.

Piccolino M & Gerschenfeld HM (1980). Characteristics and ionic processes involved in feedback spikes of turtle cones. *Proc R Soc Lond B* **206**, 439–463.

Protti DA, Flores-Herr N & von Gersdorff H (2000). Light evokes Ca^{2+} spikes in the axon terminal of a retinal bipolar cell. *Neuron* **25**, 215–227.

Rabl K & Thoreson WB (2002). Calcium-dependent inactivation and depletion of synaptic cleft calcium ions combine to regulate rod calcium currents under physiological conditions. *Eur J Neurosci* **16**, 2070–2077.

Sakitt B (1975). Locus of short-term visual storage. *Science* **190**, 1318–1319.

Sakitt B (1976). Psychophysical correlates of photoreceptor activity. *Vision Res* **16**, 129–140.

Sakitt B & Long GM (1979). Spare the rod and spoil the icon. *J Exp Psychol Hum Percept Perform* **5**, 19–30.

Thoreson WB & Burkhardt DA (1991). Ionic influences on the prolonged depolarization of turtle cones in situ. *J Neurophysiol* **65**, 96–110.

Thoreson WB, Stella SL Jr, Bryson EI, Clements J & Witkovsky P (2002). D2-like dopamine receptors promote interactions between calcium and chloride channels that diminish rod synaptic transfer in the salamander retina. *Vis Neurosci* **19**, 235–247.

Torre V, Matthews HR & Lamb TD (1986). Role of calcium in regulating the cyclic GMP cascade of phototransduction in retinal rods. *Proc Natl Acad Sci U S A* **83**, 7109–7113.

von Gersdorff H & Matthews G (1996). Calcium-dependent inactivation of calcium current in synaptic terminals of retinal bipolar neurons. *J Neurosci* **16**, 115–122.

Wu SM (1987). Synaptic connections between neurons in living slices of the larval tiger salamander retina. *J Neurosci Methods* **20**, 139–49.

Xu JW & Slaughter MM (2005). Large-conductance calcium-activated potassium channels facilitate transmitter release in salamander rod synapse. *J Neurosci* **25**, 7660–7668.

Yang XL & Wu SM (1996). Response sensitivity and voltage gain of the rod- and cone-horizontal cell synapses in dark- and light-adapted tiger salamander retina. *J Neurophysiol* **76**, 3863–3874.

Yang XL & Wu SM (1997). Response sensitivity and voltage gain of the rod- and cone-bipolar cell synapses in dark-adapted tiger salamander retina. *J Neurophysiol* **78**, 2662–2673.

Zeise ML & Hamdorf K (1983). Two late response components in on-off ganglion cells of the frog retina: the delayed response-generated by red rods; the second off-response-generated by green rods. *Vision Res* **23**, 887–893.

Zenisek D & Matthews G (1998). Calcium action potentials in retinal bipolar neurons. *Vis Neurosci* **15**, 69–75.

Acknowledgements

Author's present address

J. W. Xu: Division of Neurology, Children's Hospital of Philadelphia, 409 D Abramsson, 3615 Civic Center Blvd, Philadelphia, PA 19104, USA.